MULTI-RADIO INTERFERENCE DIAGNOSIS IN UNLICENSED BANDS USING PASSIVE MONITORING

BY AKASH BAID

A thesis submitted to the

Graduate School—New Brunswick

Rutgers, The State University of New Jersey

in partial fulfillment of the requirements

for the degree of

Master of Science

Graduate Program in Electrical and Computer Engineering

Written under the direction of

Professor Dipankar Raychaudhuri

and approved by

____

____

____

New Brunswick, New Jersey

May, 2011

ABSTRACT OF THE THESIS

Multi-Radio Interference Diagnosis in Unlicensed Bands using Passive Monitoring

by Akash Baid

Thesis Director: Professor Dipankar Raychaudhuri

The increasing density and data rate of unlicensed band wireless devices has led to significant inter- and intra-radio interference problems. Multiple competing standards such as the IEEE 802.11b/g, Bluetooth and ZigBee, all of which operate in the 2.4 GHz ISM band, can interfere with each other when used in typical indoor environments, potentially causing significant performance degradation. This thesis aims to characterize different types of heterogeneous interference in the 2.4 GHz unlicensed band and develop techniques to diagnose interference related problems using passive monitoring. The first part of the thesis presents detailed experimental results (using the ORBIT radio grid testbed) to quantify the effects of such interference in representative small office and home (SOHO) environment. In particular, different topologies, traffic loads and number of interfering devices are emulated to show the impact of multi-radio interference and to characterize each kind of interference. The second part of the thesis describes a cross-layer, multi-radio interference diagnosis framework (called "spectrum MRI") which aims to classify and diagnose multi-radio interference problems using heuristic and model-based methods. Validation experiments show that broad auto-classification of multi-radio interference in terms of congestion, slow links, inter AP interference and Bluetooth interference is possible using heuristic algorithms and passive monitoring.

Acknowledgements

I would like to take this opportunity to thank my advisor Prof. Dipankar Raychaudhuri for his guidance, motivation and constant encouragement. I have always been inspired by the simplicity of his logic, his acute engineering insights and the relevance of his advice - technical and otherwise.

I am also indebted to the people with whom I worked in due course of this thesis - Dr. Sanjoy Paul for sharing his broad range of ideas around this project, Ivan Seskar for answering endless series of questions on ORBIT and for his practical insights, and Dr. Suhas Mathur, for his constant guidance on this project and on the art of academic research.

Also, I would like to thank Prof. Roy Yates and Prof. Narayan Mandayam for being a part of my thesis committee and for their invaluable comments and insights.

Table of Contents

Abstract ii

Acknowledgements iii

List of Tables vi

List of Figures vii

1. Introduction 1

1.1. Related Work 4

2. Multi-radio Interference Experiments 7

2.1. Emulation Methodology 7

2.2. Slow Co-channel link in 802.11 8

2.3. 802.11-Bluetooth Interference 9

2.3.1. Co-located 802.11b/g and Bluetooth 10

2.3.2. Effect of Autorate on Bluetooth-802.11 Interference 11

2.4. Complex Multi-radio Scenarios 12

3. Network Measurement Techniques 15

3.1. 802.11 Promiscuous Mode Sniffing 15

3.2. Bluetooth Spectrum Sensing 16

3.3. Bluetooth Sniffing 17

3.4. ZigBee Channel Sniffing 17

3.5. Spectrum Analyzer 18

3.6. Device-side Logs 18

3.7. Wired-end Information 18

4. Interference Diagnosis Framework 21

5. Detailed Case Study: Interference to HD Video Streams 23

5.1. Topology Setup 23

5.2. Classification Parameters 25

Bluetooth Interference: 26

Channel Congestion: 27

Slow link on Same AP: 27

Slow link on Other AP: 27

5.3. Threshold Selection 27

5.4. Experimental Verification 28

6. Conclusions and Future Work 30

References 32

List of Tables

2.1. Throughput (Mbps) of Link 1 & Link 2 under different rate options for Link 2. Link 1 rate is set to maximum. 9

2.2. 802.11b & 802.11g Throughput (Mbps) with a Bluetooth interferer located at varying distance (meters) 10

2.3. Link Throughput (Mbps) with and without autorate enabled for different topologies 12

2.4. Traffic configurations of the links used in the topology of figure 2.4 . . . 13

5.1. Diagnosis Output for the proposed heuristic algorithm over different interference cases 29

List of Figures

1.1. 802.11, Bluetooth and ZigBee Channels in the 2.4 GHz ISM Band . . . 2

2.1. Topology showing the effect of a co-channel slow link 9

2.2. Throughput(Mbps) of 802.11 link at varying distances with co-located Bluetooth transmitter 11

2.3. Topology for autorate effect 12

2.4. Multi-radio Interference Topology 13

2.5. Throughput of links in topology of Figure 2.4 as percentage of their nominal value for cases when: (a) Only 802.11 links are active, (b) All 802.11b and Bluetooth links are active, (c) All 802.11g and Bluetooth links are active, (d) All links are active, ... 14

3.1. Bluetooth piconet discovery using narrow band spectrum sensing (a) 8 Mhz wide spectrogram showing Bluetooth packets, (b) Piconet Classification based on start times of Bluetooth packets (Best viewed in color) 19

3.2. Bluetooth sniffer table snapshot 20

4.1. System Level Model 22

4.2. The OML data collection framework showing the server-client architecture 22

5.1. Representative topology for Video Streaming Example 24

5.2. Interference Diagnosis Regions on the Occupancy vs Retransmission plot. (*Requires Secondary Test) 26

5.3. Snapshot of the link table showing main columns 26

Chapter 1

Introduction

The evolution of wireless protocols and access technologies for the unlicensed bands has led to the rapid proliferation of consumer grade wireless devices that require little or no spectrum configuration by end users. The choice of the unlicensed band for tetherless personal communications devices such as laptops, wireless speakers, sensors & alarm systems, short range communications between devices such as cell phone and computers, and even, media systems such as set top boxes, is a direct consequence of the the ease with which such a system can be deployed and used, by virtue of being in the unlicensed regime. This has meant that over the last few years, the density of wireless devices utilizing spectrum in the unlicensed bands has constantly gone up. Unfortunately, this has also meant that the unlicensed band is becoming interference limited, and in many cases, overcrowded with multiple radio access technologies competing for common spectrum. For example, the popular 802.11 standard, the Bluetooth standard and the ZigBee standard, all share the same chunk of radio spectrum, as shown in Figure 1.1, in addition to emitters such as cordless phones and leaking microwave ovens, also in the same band.

Each of these wireless access technologies have their own specifications for modulation, power control, rate control, networking and mediating access to the wireless medium with other terminals *of the same type*, but not across different standards. For example the 802.11 standard specifies a set of rules in the form of a MAC protocol that allows two or more terminals on the same 22 MHz channel to share the spectrum efficiently. However, the Bluetooth and ZigBee standards do not understand the 802.11 protocol and vice-versa. Furthermore, one radio-access standard consists of radios that are tuned to transmit and receive units of data that only correspond to that

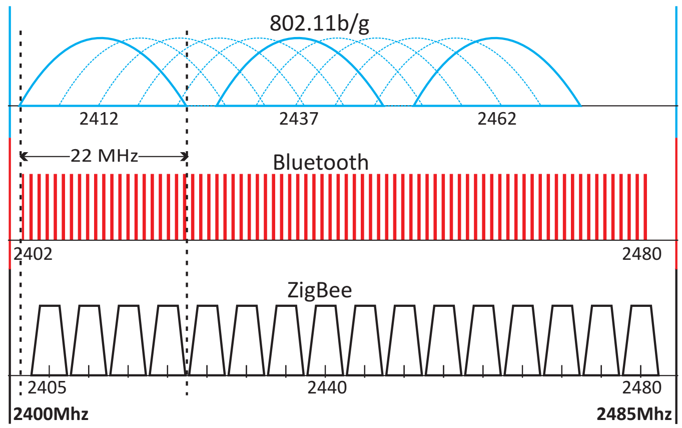

Figure 1.1: 802.11, Bluetooth and ZigBee Channels in the 2.4 GHz ISM Band

standard, and therefore, a transmission by a different type of radio is treated simply as noise, when it is actually interference from another family of radios. The current generation of radio standards does not incorporate the intelligence of coordination between different radio access families. In this work we show that depending on physical topology, transmit power levels and traffic requirements, this can lead to moderate to severe performance degradation in the QoS of one or more links. We refer to this as the multi-radio interference problem.

In the debate over how best the spectrum resource should be utilized, the greatest fear among skeptics of the unlicensed spectrum model is that spectrum, if left completely unregulated, can quickly lead to a tragedy of the commons [1]. This is not a completely theoretical concern - such a tragedy has in fact occurred in the past, for instance in the case of citizens band radio [2], where lack of regulation led to such severe overcrowding that poor user experience caused users to be driven away from using the band completely.

In this thesis we study the multi-radio interference problem in detail, focusing on the performance loss under various scenarios, and we put forward the claim that in many cases it is possible to diagnose interference problems in a multi-radio environment by passive observation of symptoms that interference problems produce. Our goal is to build a system using one or more *monitors* that collect data passively and aggregate their observations that are fed into a database for subsequent processing by suitable algorithms for problem diagnosis. If a control channel is available between this system and the wireless terminals causing interference, the system can then close the loop by sending control signals recommending an alternate configuration, for example a recommendation to move to a different channel. Even without such a control channel, the system might recommend an alternate configuration to a human in the loop. We believe that a low-cost system that can monitor transmissions on multiple radio interfaces can dramatically improve performance degradations arising out of multi-radio co-existence and lead to much more efficient use of the spectrum.

Let us take a few concrete examples to illustrate the multi-radio interference problem.

- Example 1: Consider a VoIP application running over an 802.11 link with the last hop to the user on a Bluetooth link. In this example, a Bluetooth transmitter and 802.11 receiver are co-located. As we will show, even with the lower power of Bluetooth signals, a co-located Bluetooth transmitter and 802.11 receiver can lead to considerable performance degradation.

- Example 2: A high speed 802.11g streaming video running in a home or office environment can create a shortage of channel availability and starve any other device on the same spectrum, such as a ZigBee sensor for a fire or theft alarm.

- Example 3: A high speed video link for a set-top box to a television and a set of Bluetooth speakers in the same vicinity will create mutual interference for one another and due to the streaming nature of both applications, an easily perceptible drop in quality will result.

- Example 4: An 802.11b link set to operate at a rate of 1 Mbps can severely starve a nearby high-speed 802.11g link that is set to operate on 54 Mbps. This is a backward compatibility problem. The 802.11b link effectively hogs the channel for a large fraction of time, thereby slowing down the 802.11g link.

The nature of unlicensed spectrum makes the problem of interference even more complicated because terminals contending for the same spectrum in a given geographic area may belong to disparate entities. For instance, the performance of an 802.11 link in one home may be adversely affected by the use of a cordless phone or a leaking microwave oven in the neighboring home. This type of loss in throughput due to interference is very common and is usually realized only when there is a complete loss in connectivity, even though there is always a substantial loss in performance in most cases. Monitoring the spectrum for tell-tale signs of interference-related problems in wireless networks can help mitigate poorly configured services and to pinpoint the cause of a poorly performing link.

The rest of this thesis is organized as follows. In chapter 1.1, we present prior work in the area of interference mitigation and wireless network diagnosis that is relevant to our work. In chapter 2 we present results from our experiments on characterizing the effect of interference in multi-radio scenarios. Chapter 3 highlights some of the tools used for collecting diagnostic information from various sources. Following this, in chapter 4 we outline our interference diagnosis framework which can help in interference classification and diagnosis in a complex heterogeneous radio environment. A specific example of problem diagnosis using the proposed framework is given for an indoor 802.11g video link. Chapter 6 concludes the thesis and provides an overview of the future direction of our research.

1.1 Related Work

As radio standards in the unlicensed bands have evolved over the years, a number of studies on inter-radio interference have been conducted typically following an approach that seeks to characterize one standard versus another. These studies have most often involved interference modeling and analysis of the impact of one type of radio on the other. For example [3] and [4] analyze the impact of Bluetooth on 802.11b/g and suggest some techniques to improve co-existence between these two standards. Similarly, [5] provides a detailed analytical model for interactions between ZigBee and 802.11 and between ZigBee and Bluetooth. In a complex multi-radio environment having simultaneous interactions of several competing wireless standards, the approach of modeling and analysis becomes much harder. The IEEE 802.15.2 standard [6] addresses some of the issues in this regard and presents recommended practice for the co-existence of WLAN and WPAN devices.

A related area of research focuses on the more fundamental causes and effects of interference on PHY and MAC layer performances with the aim of designing techniques to overcome the problems involved (for example [7]). However, the 802.11 standard has received most of the attention in such studies, and the prime focus has overwhelmingly been on 802.11 wireless links being the victim of the interference. Stranne *et al.* [8] goes a step further to derive closed-form throughput expressions by creating an analytical framework for interactions between heterogeneous radios using such physical layer models. More recently, there has also been work on designing techniques to facilitate co-existence between multiple radios using the idea of a common control channel [9]. Our work, in contrast to previous studies of heterogeneous radio interference, focuses on the diagnosis aspect. Within a complex radio environment, there are various practical issues that limit the use of shared spectrum knowledge under the present standards. As a way out, we study the question of whether it is possible to infer and classify interference problems with the aim of building a working system for diagnosis of such problems in an environment with multiple heterogeneous radios.

The area of network diagnosis and management is closely related to this work and we provide a brief overview of some of the relevant studies in this field below. Due to the wide-scale popularity and infrastructural importance of the 802.11 WLAN standard, most work in this domain, apart from those on wired networks, has focussed on solving issues within this standard. Cheng *et al.* [10], for example, provides details on an elaborate cross-layer trace collection and analysis system to address issues ranging from configuration problems to interference related problems. Similar work in [11] focuses on the framework for detecting a wide range of faults and security issues typical to the WLAN systems. Some other approaches for 802.11 WLAN diagnosis include a structural and behavioral model based system [12], RF energy duration based fault detection [13], distributed physical layer anomaly detection [14], and fault diagnosis using signal error rate and RSSI parameters [15]. With the pronounced emphasis on 802.11 systems as the point of focus, the research in [10] - [15] clumps all types of interference and noise as seen by an 802.11 receiver into a single category, choosing not to differentiate between transmissions of other radios and background noise. It is easy to see that an important reason behind this 802.11-centric view of the unlicensed spectrum has been the motivation for makers of management software for WLAN systems to improve the performance of their systems.

The goal of our system on the other hand, is to improve performance of the entire system, consisting of multiple heterogeneous radios. Research issues for this work therefore also include the development of tools and a framework to collect multi-radio, cross-layer information about the radio environment and techniques for intelligent classification and diagnosis algorithms based on such a framework.

Chapter 2

Multi-radio Interference Experiments

In this section, we present examples of some typical multi-radio interference problems in home networks. We classify the interference measurement experiments into the following categories:

- Intra 802.11 Interference
- Inter-radio Interference
  - 802.11-Bluetooth Interference
  - 802.11-ZigBee Interference
  - Bluetooth-ZigBee Interference
- Complex Multi-radio Interference

2.1 Emulation Methodology

All the experimental evaluations described in this section were conducted on the ORBIT testbed [16] which consists of 400 small form-factor PCs placed in a 20 x 20 regular grid with an inter-node separation of about 3ft, spanning a total area of 3600 sq. ft. Each of these nodes is equipped with two IEEE 802.11a/b/g wireless interfaces, with 40 nodes also equipped with Bluetooth dongles and 30 nodes also equipped with 802.15.4 TelosB motes [17]. The Iperf tool [18] is used for throughput measurement of TCP and UDP data in both 802.11 and Bluetooth radios and a customized ZigBee traffic generator built on the TinyOS platform [19] is used for performance measurement on the ZigBee nodes. The throughput measurements in each of the experiments described in this section were averaged over ten or more readings spread in time and location inside the

ORBIT grid to remove random effects of environmental changes and device specific variance. Unless otherwise mentioned, all the 802.11 nodes in our experiments were operated on Channel 1 which did not have any external interference as confirmed by a spectrum analyzer. In the following sections, we identify and quantitatively analyze some commonly occurring multi-radio interference problems:

2.2 Slow Co-channel link in 802.11

When two or more 802.11 b/g links co-exist on the same channel, the slower links have a higher channel occupancy time causing the high rate links to undergo more backoffs and thus suffer a large drop in throughput. To quantify this effect, three cases of single link interference are emulated as shown in Figure 2.1. In all the three cases, the data-rate of Link 1 is set to the highest (11 Mbps for 802.11b and 54 Mbps for 802.11g) while the rate of Link 2 is changed in steps. All links in this experiment carry saturation TCP traffic with a buffer size of 8 KBytes. From Table 2.1, we observe a substantial drop in Link 1 throughput when the interfering link (Link 2) data-rate drop downs from 11 Mbps to 1 Mbps in all the three cases. This drop is about 32% in case of 802.11b-802.11b interference and 53% in case of 802.11g-802.11g interference.

The throughput loss increases with the number of interfering slow links and decreases with the distance between the interfering transmitter and the high rate receiver. From a practical point of view, this scenario is very common and presents itself in a number of ways. For example if an old laptop with a slow 1 Mbps 802.11b radio link is connected to an AP, all the other clients connected to that AP suffer a loss in throughput because of it. Variation in bit-rate due to signal quality variations across a home because of propagation through walls, etc. is quite typical. In such a case, the link with reduced rate affects other clients even though they might have a good signal reception from the AP. The rate reduction can also be brought about if there is some sort of local interference (like Bluetooth) near one of the links. The affected link then starts an automatic rate reduction scheme which in turn can cause the throughput of all the other links on the same channel to go down.

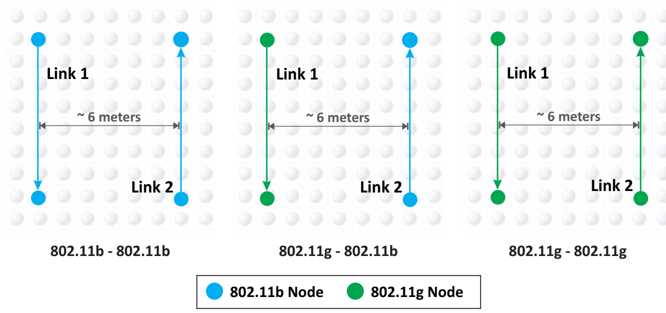

Figure 2.1: Topology showing the effect of a co-channel slow link

Configuration	Link	1 Mbps	2 Mbps	5.5 Mbps	11 Mbps
11b-11b	Link 1	1.19	1.79	2.89	3.76
	Link 2	0.63	1.14	1.92	2.87
11g-11b	Link 1	17.60	20.60	22.32	25.10
	Link 2	0.36	0.50	0.78	1.74
11g-11g	Link 1	9.67	12.72	14.70	17.91
	Link 2	0.62	1.34	2.42	4.66

Table 2.1: Throughput (Mbps) of Link 1 & Link 2 under different rate options for Link 2. Link 1 rate is set to maximum.

2.3 802.11-Bluetooth Interference

One of the most common type of and widely studied inter-radio system is the 802.11-Bluetooth pair. With an increasing use of devices of both standards, co-existence of these devices is a major concern in the unlicensed 2.4GHz band. The most severe 802.11-Bluetooth interference is observed in the co-located case where the Bluetooth and 802.11b/g radios are located on the same physical device such as smart phones and laptops. At such distances, a transmission on any of the roughly 22x1 Mhz Bluetooth channels that overlap with a 802.11 channel will cause a packet error for the 802.11 transmission. Though there has been an introduction of Adaptive Frequency Hopping (AFH) starting from Bluetooth version 1.2, the percentage of devices utilizing this technique is very small [20]. Also a potential interference issue that the AFH introduces is the intra-Bluetooth interaction problem. In the presence of 802.11b/g networks in multiple channels, the AFH algorithm forces the Bluetooth to hop within a small number of frequencies, thus creating a high probability of collision if there are multiple number of such AFH Bluetooth devices. To illustrate all these interference related

Distance	802.11b	802.11g
0.25m	5.64	10.20
3m	5.79	11.05
6m	5.82	11.80
8m	6.15	13.90
11m	6.13	13.76
13m	6.35	13.69
16m	6.27	14.87
19m	6.42	15.40
No interference	6.61	17.65

Table 2.2: 802.11b & 802.11g Throughput (Mbps) with a Bluetooth interferer located at varying distance (meters)

problems, the following two simple case experiments were performed:

2.3.1 Co-located 802.11b/g and Bluetooth

Dual radio nodes were used to emulate a co-located case in which the distance between the 802.11b/g and Bluetooth radios is about 25cm and the transmit power is 18dBm and 4dBm(Class 2 device) for 802.11b/g and Bluetooth respectively. To create a worst-case interference scenario in this topology, the Bluetooth transmitter and the co-located 802.11b/g receiver operate concurrently. The 802.11 transmitter is located at varying distance which varies the received power levels at the receiver. TCP traffic is pushed through the 802.11b/g link with the rate set at 11 Mbps for 802.11b and 24 Mbps for 802.11g. The Bluetooth interferer carries a 512 Kbps UDP load with a datagram size of 1 KB. From the observed throughput numbers in Figure 2.2 we can see that the impact of Bluetooth is more on 802.11g link with a steeper drop with distance. And when the 802.11g transmitter and receiver are separated by a distance of 15 meters or more, the 24 Mbps connection cuts down to less than 3 Mbps.

Apart from the co-located case, in order to quantify the effect of distance between Bluetooth interferer and 802.11 receiver, the same experiment is repeated with varying this distance and the throughput for 802.11b and 802.11g cases are reported in Table 2.2. As before, we can see an almost constant drop for 802.11b and a gradual deterioration in the case of 802.11g but the percentage drop goes down as the Bluetooth interferer moves away from the 802.11b/g transmitter.

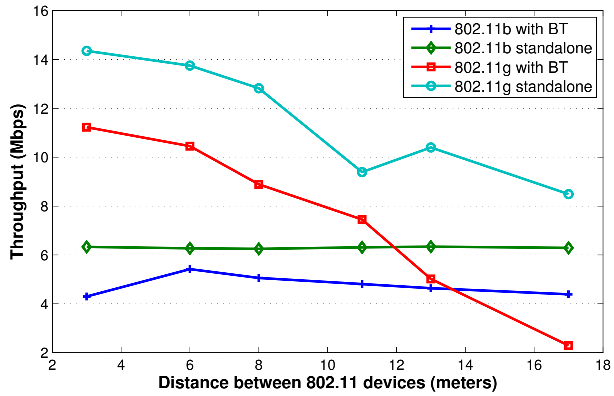

Figure 2.2: Throughput(Mbps) of 802.11 link at varying distances with co-located Bluetooth transmitter

2.3.2 Effect of Autorate on Bluetooth-802.11 Interference

To study the role of automatic rate selection in presence of Bluetooth interference, we measure the throughput (using TCP traffic at 11 Mbps) of a 802.11b link with and without autorate enabled in the three configurations shown in Figure 2.3. The distance between the transmitter and the receiver for both 802.11 and Bluetooth nodes is fixed at 4 meters in each case. While there has been significant research to design optimum automatic rate fallback algorithms in WLAN, for our demonstration purpose we use the autorate feature in the MadWifi driver, which implements the Onoe bit-rate selection algorithm. From the throughput numbers shown in Table 2.3 we can clearly see that rate reduction in such a scenario causes longer collision windows and thus lower throughput in 802.11b. With autorate option enabled in most laptop 802.11b/g cards, this presents a very common example of a configuration problem that causes loss in throughput. An important point here is that autorate algorithms have been proven to substantially help in solving contention based problems in case of intra-radio interference and noisy environments and thus this presents a case to have a selective algorithms that factor in the kind of interference into its algorithm.

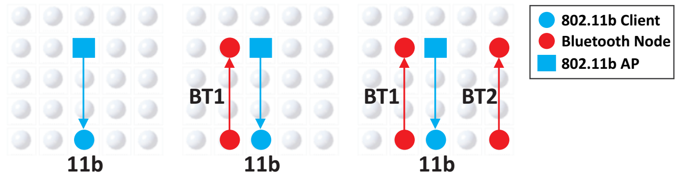

Figure 2.3: Topology for autorate effect

Topology	Rate set at 11Mbps			Using Autorate Option		
	11b	BT1	BT2	11b	BT1	BT2
Only 11b	5.40	–	–	4.92	–	–
11b & BT1	3.95	0.25	–	1.92	0.25	–
11b, BT1 & BT2	2.81	0.24	0.63	0.42	0.30	0.69

Table 2.3: Link Throughput (Mbps) with and without autorate enabled for different topologies

2.4 Complex Multi-radio Scenarios

As a final example of multi-radio interference, we emulate a complex small office environment consisting of multiple 802.11b, 802.11g, Bluetooth and ZigBee radios distributed throughout the premises. As is shown in Figure 2.4 an 802.11b node on channel 1 forms the main access point to which four clients are connected. Two additional 802.11g links on channels 1 and 11 respectively support point to point devices such as set-top box to TV or projector links. A fifth 802.11b link on channel 11 emulates point to point file transfer in this scenario. As is common in commercial premises, there are neighboring APs within the interference region of the environment, here depicted by an 802.11g AP on the top-left with two clients. Some three Bluetooth constant bit rate transmissions add to the radio clutter with one of the Bluetooth nodes being co-located with the 802.11g node. A number of low cost ZigBee sensors form a part of the security/temperature control infrastructure and relay periodic readings to a central ZigBee concentrator in this scenario.

The aim of this experiment, consistent with the rest of the section, is to get raw throughput numbers in order to quantify the interference problems. The topology, number and density of the radios is typical of an office environment where a myriad of complex interferences gives rise to loss in throughput of the entire system. In some cases the the loss in throughput is not inherently visible due to the low data rate applications

Links	Traffic Configuration
B1, B2, B3, B4	Saturation TCP connection with 11 Mbps data rate
B5	Constant Bit Rate UDP connection with 10 Mbps offered load
G1, G2, G3, G4	Saturation TCP connection with 54 Mbps data rate
BT1, BT2, BT3	Constant Bit Rate UDP Connection with 512 Kbps offered load
All ZigBee Nodes	Periodic 50 Byte data transfer every 100ms at 250 Kbps

Table 2.4: Traffic configurations of the links used in the topology of figure 2.4

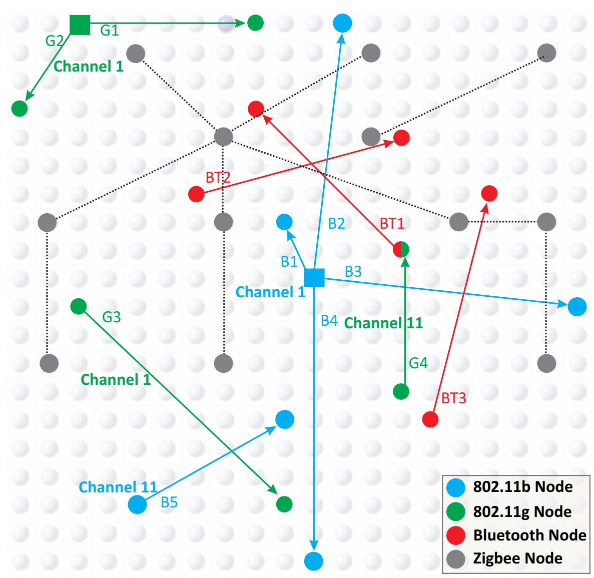

Figure 2.4: Multi-radio Interference Topology

that these links generally support but with a gradual increase in both the density of radio devices as well as the data rate of the applications, there is a potential problem that exists in such a scenario. Here we do not emulate the actual traffic characteristics but to gather info on the throughput loss, we form a saturation load on the links with the exact configurations listed in Table 2.4

Figures 2.5(a) - 2.5(d) show some of the throughput results from the multi-radio experiments under different configurations where the nominal throughput is defined as the no-interference throughput for each link. While the numbers do not completely reflect practical scenarios since the traffic load is different for different applications,

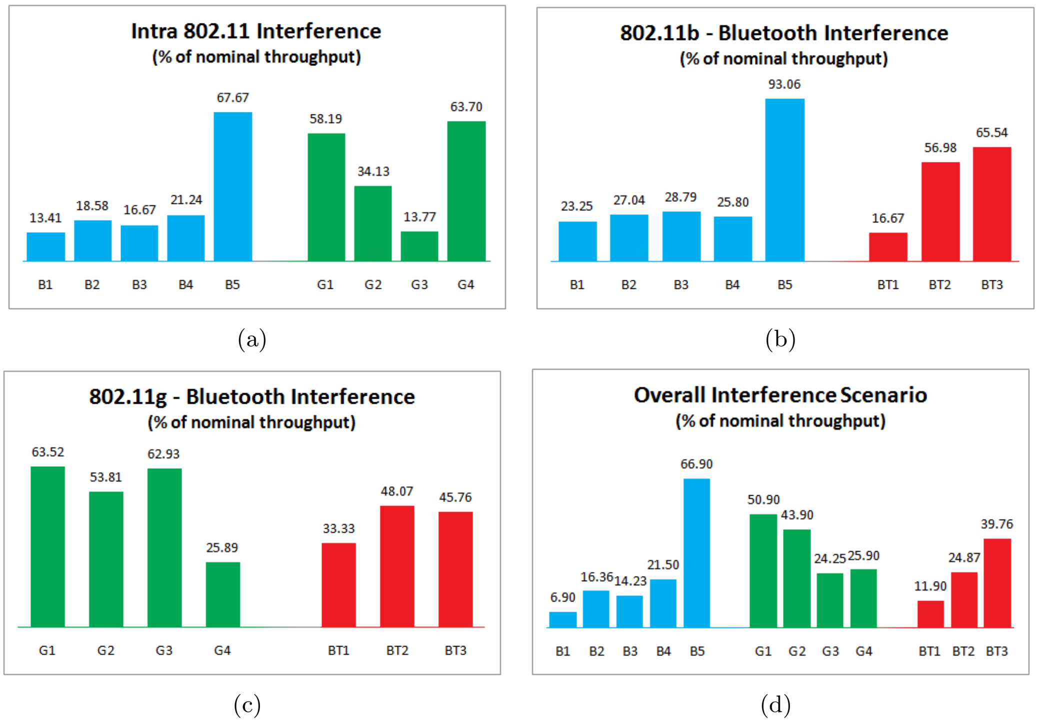

Figure 2.5: Throughput of links in topology of Figure 2.4 as percentage of their nominal value for cases when: (a) Only 802.11 links are active, (b) All 802.11b and Bluetooth links are active, (c) All 802.11g and Bluetooth links are active, (d) All links are active,

yet it shows a comprehensive picture of the kind of inter-radio interference that we are addressing in this thesis. For example Figure 2.5(d) clearly suggests that when all the links are active a drop of more than 50% is observed for most links in the network. For this case, we also measured the percentage of packets received by the ZigBee concentrator from all the other nodes in a 5 second interval (all ZigBee nodes are configured to channel 11 of the 802.15.4 standard in this experiment). This number goes down from 83% in case of no-interference case to less than 2% when all the other links are turned on, suggesting a very important problem of high importance fire, theft or sensory information being obstructed by traffic on other radios. The aim of our research is to identify such cases of interference related throughput reduction and to diagnose the exact cause as far as possible.

Chapter 3

Network Measurement Techniques

Given the complex heterogeneous radio environment, as described in the previous sections, the effect of inter-radio and intra-radio interference is manifested at both the physical/data link layers as well as the transport/application layers. As such, the study of such interferences requires a multi-radio, cross-layer measurement system that employs different data collection techniques suited to different kinds of radios. The experiments described in the previous section used some *active methods* to measure link quality and throughput which involved test transmissions and direct throughput logging on each client. While these active measurements comprehensively show the effect of interferences, it is not a pragmatic method to diagnose and classify interferences in a complex environment since we do not have access to run client side applications in most real cases. As such we employ some *passive methods* for non-intrusive sniffing of ongoing transmissions.

3.1 802.11 Promiscuous Mode Sniffing

Wireless monitoring of 802.11b/g networks has been employed for both network usage collection [21] as well as security and threat management [22] as it provides an inexpensive and scalable insight to the network traffic. For our purpose of fault diagnosis, it provides a myriad of helpful information, for example, RSSI, logical topology, network traffic, number of retransmissions, network load, etc. A modified application of the tcpdump tool [23] using the packet capture library (libpcap) is used in our application that logs the headers of all packets received on the wireless interface card of the node and ports this data to the central database. The customized application also appends client and server timestamps denoting the time of reception of a packet by the monitor and the central server respectively. Using these fields, multiple logs of the same packet received by different monitor nodes are purged, keeping only the timestamp and RSSI from these repeat traces. Channel selection and dwell time on a channel while sniffing multiple channels is controlled by the central server.

3.2 Bluetooth Spectrum Sensing

The Bluetooth protocol incorporates a frequency hopping scheme using a sequence of 1 Mhz wide channels selected from the 79 channels in the ISM band. The dwell time for each hop is 1, 3 or 5 time slots, with each time slot being 625 μs in length. This inherent hopping mechanism makes Bluetooth monitoring a much harder problem compared to 802.11 or ZigBee standards. Improving upon the approach in [24], we use limited bandwidth spectrum snapshots to ascertain the number of Bluetooth piconet that are active in the surrounding and estimate the amount of traffic by counting the number of packets received.

Figure 3.1(a) shows the spectrogram observed from a narrow band energy capture using the GNURadio software with the USRP hardware platform. Due to hardware limitations, we can only observe a maximum of 8 Mhz of the spectrum which corresponds to 8 Bluetooth channels, in this case from 2433 Mhz to 2441 Mhz. The Bluetooth packets can be isolated from this spectrogram using time and frequency limited windows to identify high energy regions. Once we have all the Bluetooth packets, a time binning approach, as specified in [24], is used to find the number of piconets. The basic algorithm of this approach involves putting the start time of each of the detected packets into 25 μs bins and then using the fact that transmissions from the same piconet are always integral number of time slots apart. Figure 3.1(b) shows the automatic classification of the packets into packets from different piconets by this algorithm. A similar approach of using the USRP platform to sense the environment was used in [25], however the main aim in that work was to localize the transmitters compared to identifying the type of transmission in our case.

While it is not a detailed view of the Bluetooth transmissions, this method provides a simple estimate of the number of active Bluetooth transmissions and their traffic load (based on the number of packets observed). This information when used along with 802.11 packet sniffers, for example, can give a clue to a Bluetooth-802.11 interference problem if a simultaneous transmission followed by MAC retransmissions is observed. A more evolved algorithm than the one described here can be developed to automate the process of real-time spectrum sensing and Bluetooth detection with time synchronization with other kind of sensors. As part of our continuing research, we are working on algorithms to adaptively change the energy thresholds and frequency band of operation, and also on creating a time synchronized real time system that can feed the Bluetooth packet sensing data to a central database.

3.3 Bluetooth Sniffing

While the spectrum sensing method provides an estimate of the number of Bluetooth piconets and the timing information on packet transmissions, a much more detailed view can be gathered by sniffing on an active piconet and following the frequency hops. Once the sniffing device is connected to the Bluetooth Master, it can tabulate the frequency of operation, timestamps, packet type, underlying baseband packet header and more information on all the transmissions on that piconet. A simple snapshot of the Bluetooth sniffer is given in Figure 3.2. Commercial products like the FTS4BT Bluetooth Protocol Analyzer & Packet Sniffer [26] enable more advanced features of real-time capturing, filtering and piconet selection.

3.4 ZigBee Channel Sniffing

We employ a passive frequency-hopping listener application built upon the TinyOS platform to log and aggregate the packets received over the ZigBee interface. These are then ported to the OML server keeping the tables in sync with other monitors.

3.5 Spectrum Analyzer

A low-cost coarse resolution spectrum analyzer like [27] can provide a means to detect other sources of RF emissions, for example that from cordless phones, leaking microwave ovens, etc. Since these devices are commonplace in a SOHO environment, we employ this additional monitor to diagnose such interference problems.

3.6 Device-side Logs

Interference being a receiver side phenomenon, can be best detected from the user device involved in the transmission. As such, we have an optional device side logging mechanism which records the changes in throughput, delay and received power.

3.7 Wired-end Information

With some prior knowledge about the devices, the wired-side logs from the AP, for example, can provide information about the logical topology of the system which helps the diagnosis algorithm to narrow down on the interfering links.

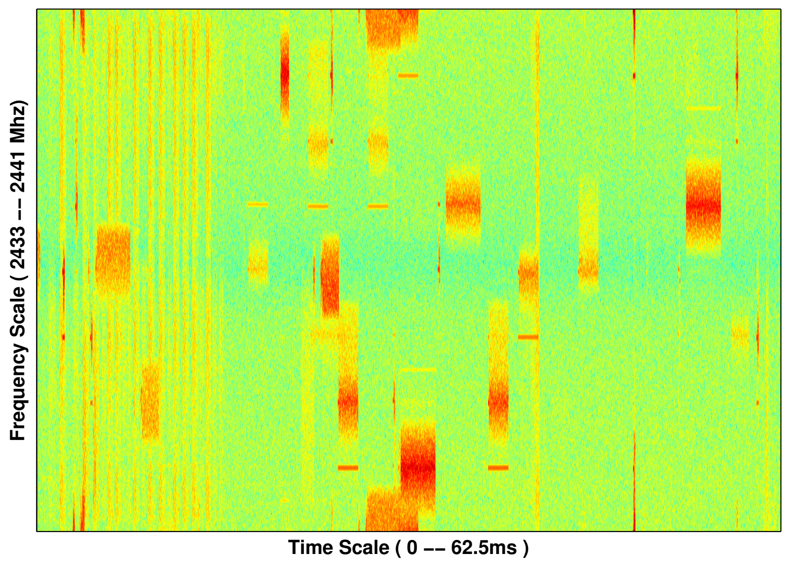

(a)

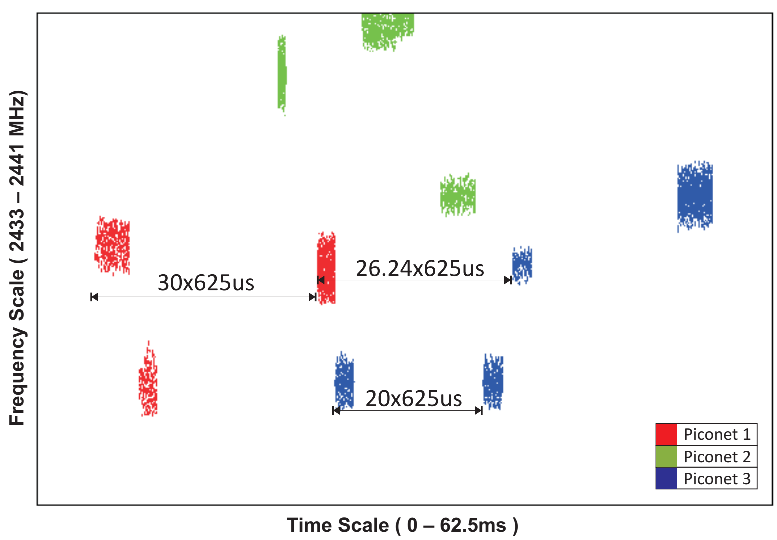

(b)

Figure 3.1: Bluetooth piconet discovery using narrow band spectrum sensing (a) 8 Mhz wide spectrogram showing Bluetooth packets, (b) Piconet Classification based on start times of Bluetooth packets (Best viewed in color)

Fra...	CLK	Chan	TYPE	LLID	SEQN	ARQN	Len	Fr...	Delta
3,374	0x0bacbabe	48	DH5	L2CAP	1	0	323	331	00:00:00.0025
3,375	0x0bacbaca	0	DH5	Continuation	0	0	339	347	00:00:00.0037
3,376	0x0bacbad6	36	DH5	Continuation	1	0	339	347	00:00:00.0037
3,377	0x0bacbae2	22	DM3	Continuation	0	0	42	50	00:00:00.0037
3,378	0x0bacbaea	6	DH5	L2CAP	1	0	339	347	00:00:00.0025
3,379	0x0bacbaf6	42	DH5	Continuation	0	0	339	347	00:00:00.0037
3,380	0x0bacbb0e	72	DM3	Continuation	0	0	42	50	00:00:00.0075
3,381	0x0bacbb14	51						14	00:00:00.0018
3,382	0x0bacbb16	64	DH5	L2CAP	1	0	338	346	00:00:00.0006
3,383	0x0bacbb22	58	DH5	Continuation	0	0	339	347	00:00:00.0037
3,384	0x0bacbb2e	13	DH5	Continuation	1	0	339	347	00:00:00.0037
3,385	0x0bacbb3a	52	DM3	Continuation	0	0	42	50	00:00:00.0037

Figure 3.2: Bluetooth sniffer table snapshot

Chapter 4

Interference Diagnosis Framework

We now present a framework for multi-radio interference diagnosis that uses the interference monitoring and data logging capabilities described in the previous section for intelligent interference detection and resolution. As shown in Figure 4.1, our framework consists of a central database that collects trace data using a network of time synchronized spectrum sensors that can detect 802.11, Bluetooth and ZigBee transmissions. Each of these sensors or network monitoring tools looks at the network from a different viewpoint, thus each of them add an extra dimension for the diagnosis algorithm to work with. These sensors use the Orbit Measurement Library (OML) [28] and the Orbit Management Framework (OMF) systems for collecting network traces. The OML framework consists of a client application that runs on each of the sensor node and a central server which is responsible for collection and storage of the measurements in a database. As shown in Figure 4.2, the diagnosis inference engine parses the central database and uses a decision tree based algorithm to make appropriate diagnosis on the cause of interference. There is a feedback path from the inference engine to the sensors so that measurement parameters can be changed dynamically.

While some of the techniques mentioned under network discovery tools in Figure 4.1 have been explained earlier, some others use common existing techniques to gather data. The issue of time synchronization between these varied sensors becomes important if the type of analysis required for diagnosis is correlative in nature. The use of OML, as mentioned earlier also addresses this problem by maintaining a fine grained time stamp of each packet received on each monitor. The core component of this data driven approach is the inference algorithm engine which is designed based on protocol heuristics and representative problem scenarios. For example, while performing

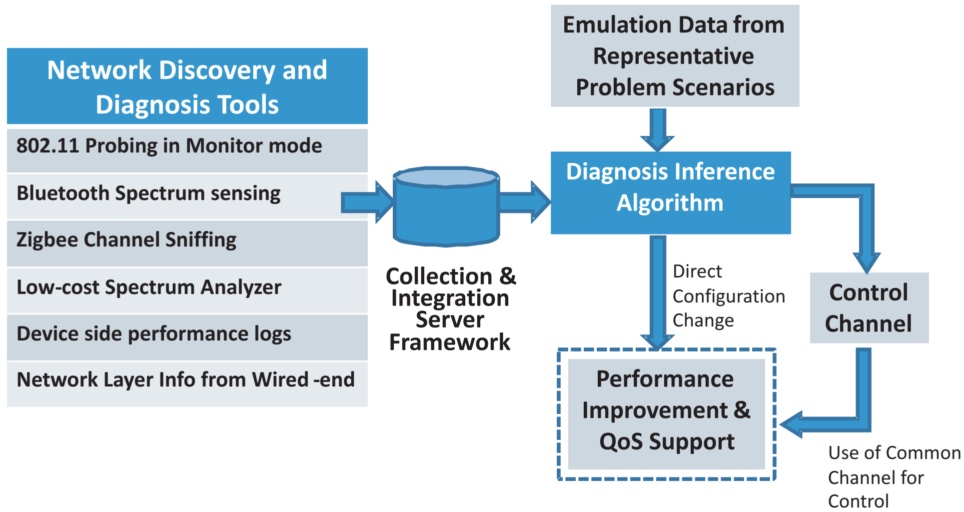

Figure 4.1: System Level Model

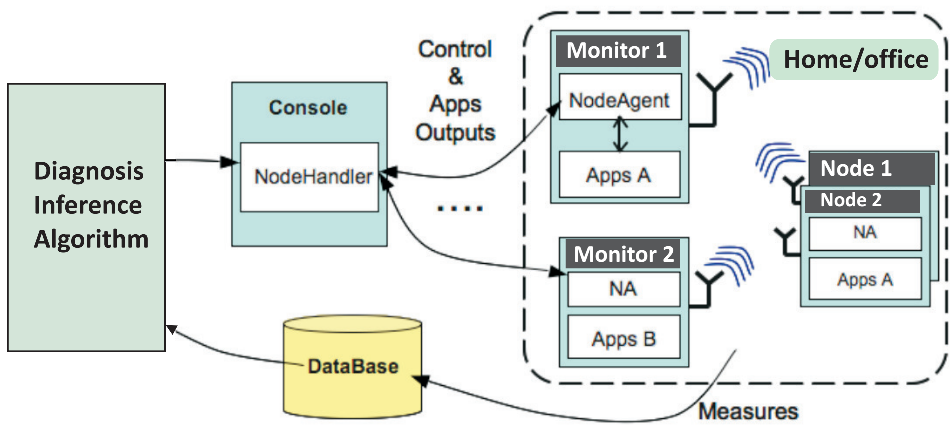

Figure 4.2: The OML data collection framework showing the server-client architecture

Bluetooth-802.11 interference experiments, we observed that the percentage of packets requiring retransmission increases substantially. Thus a possible heuristic rule to detect and diagnose such a case might involve the retransmission percentage as a parameter. This case of Bluetooth and other kinds of interferences to an 802.11 link is explained in greater detail in the next section and the main focus of the ongoing work is development of further diagnosis algorithms and identifying further parameters that can be used for that. The right way to use the diagnosis is yet another topic of research spanning the entire spectrum from user notification to common control plane architecture with fine grained control over time, frequency, rate and power of multiple transmissions.

Chapter 5

Detailed Case Study: Interference to HD Video Streams

In this section, we provide a detailed example of how the proposed data-centric approach can be used to diagnose possible interference related problems in a specific real world application - that of high-rate video transmissions. Wireless HD streaming is increasingly gaining popularity in home settings as a natural next-step after an explosion in HDTV penetration. Due to its high bandwidth and low delay requirements, this presents itself as an important problem in the SOHO environment that our work is focussed on. As mentioned in the previous sections, many different kinds of RF interference can affect the quality of the video stream, ranging from unnoticeable rate adjustments to largely unviewable video quality. As an initial case study, we define four possible interferences to a video stream in a home environment and subsequently elaborate on the key parameters that can be used to characterize and diagnose each of these problems.

5.1 Topology Setup

To emulate a small home network, we ran our experiments based on the representative topology shown in Figure 5.1. In Figure 5.1, link 1 is the main video stream, with the distance between the transmitter and receiver being close to 10 meters. The VLC application [29] is used to emulate the video link and a CBR 15 Mbps video at a transmit rate of 54 Mbps is used as the stream. The location of the 802.11 monitor operating in the promiscuous mode, as explained in Section 3, is indicated by the blue star. It is important to note here that it is a basic premise in our problem that we only have access to this passive monitor and any diagnostic algorithm that we device cannot assume the knowledge of the either the transmitter or the receiver side information on

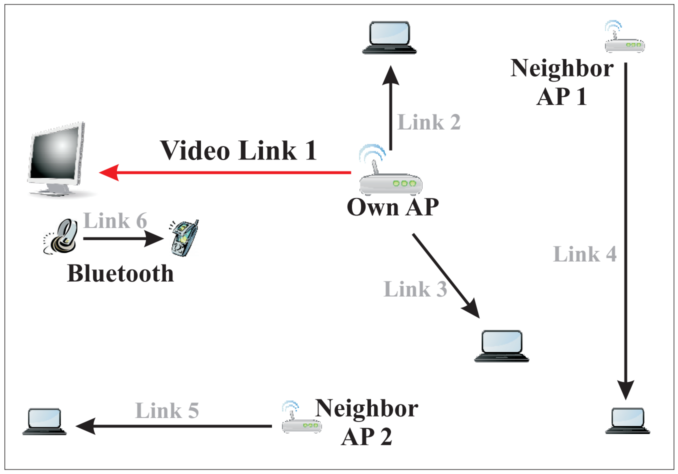

Figure 5.1: Representative topology for Video Streaming Example

any of the links.

Links 2 and 3 represent other user devices connected to the same AP and both of them generate approximately 1 Mbps TCP data traffic at 54 Mbps link speed with constant inter-departure time and Pareto-distributed packet length with mean 450 bytes. Links 4 and 5 are independent AP-client pairs that emulate neighboring links outside the home, quite commonly found in such a setting. Unless mentioned otherwise, these links carry 2 Mbps data traffic at 54 Mbps each with the same characteristics as that of links 2 and 3. There is also a Bluetooth pair close to the video receiver which carries a CBR UDP 512 Kbps on-off data stream. In the rest of this section, we work with the following four types of interferences to the video link under a reasonable assumption that only one of the four problems dominate the video quality at a given point of time:

- Bluetooth Interference
- Slow link on the same AP
- Slow link on a neighboring AP
- Channel Congestion

While this presents a small selection from the wide variety of interferers present in a home environment, all of the listed problems are very common for home networks and in this case study, we show how a passive observation of the various link transmissions can be used to filter out signatures that can be ascribed to each of these problems.

5.2 Classification Parameters

As the case with any other kind of diagnostics, in order to say 'Problem X occurred due to reason Y', we need to first identify the parameters that show the 'symptoms' of the problem and then classify the multi-dimensional parameter space with appropriate hyperplanes. After tackling a difficult problem of selecting the thresholds that define these hyperplanes, what we finally get is a segmented multi-dimensional space and the location of a link/network state in this space should indicate, with a sufficiently high probability, that either the link if healthy or has problem X1, or problem X2, and so on.

Based on these fundamentals, we found that the two most important parameters for the problems mentioned above are the per-link percentage-retransmission and the occupancy. Here we define link occupancy as the fraction of time for which this link was transmitting data and includes both primary and the retransmissions. These two and other parameters are aggregated using a variable width sliding window to avoid unrelated artifacts and reduce storage requirement. Unless otherwise mentioned, we use a 200ms averaging window with no overlap and as can be seen from a snapshot of the database in Figure 5.3, each row shows the average parameter value after averaging over all the packets received during the interval. The classification of the four problem scenarios, primarily based on these two parameters are shown in Figure 5.2 which is explained later in this section. To have an idea of the parameter values for a healthy case of nominal traffic on all interfering 802.11 links and no Bluetooth interference, the baseline operating point is marked in the figure which shows 2.8% retransmissions and link occupancy ratio of about 0.24. In addition to this baseline traffic, the effect of each of the four problems show up in slightly different ways as follows:

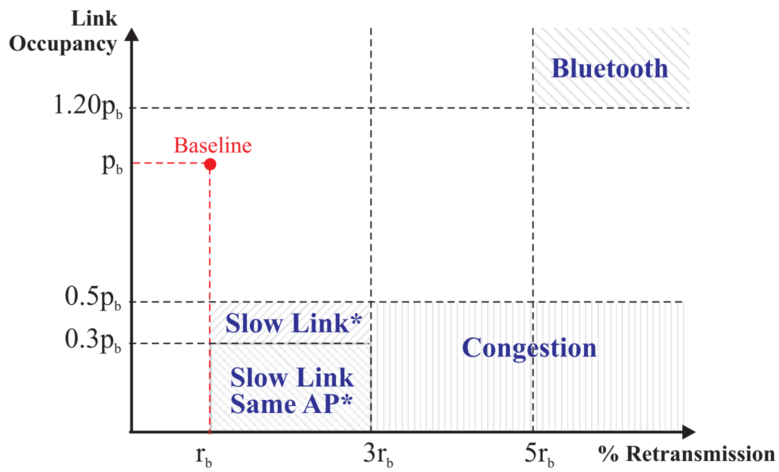

Figure 5.2: Interference Diagnosis Regions on the Occupancy vs Retransmission plot. (*Requires Secondary Test)

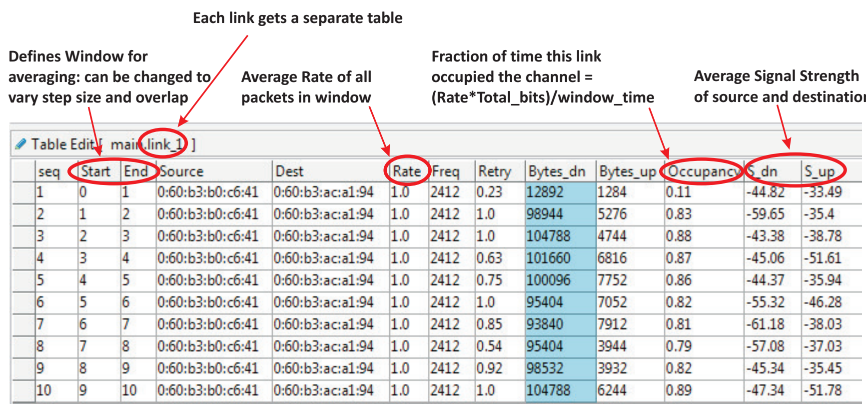

seq	Start	End	Source	Dest	Rate	Freq	Retry	Bytes_dn	Bytes_up	Occupancy	S_dn	S_up
1	0	1	0:60:b3:b0:c6:41	0:60:b3:ac:a1:94	1.0	2412	0.23	12892	1284	0.11	-44.82	-33.49
2	1	2	0:60:b3:b0:c6:41	0:60:b3:ac:a1:94	1.0	2412	1.0	98944	5276	0.83	-59.65	-35.4
3	2	3	0:60:b3:b0:c6:41	0:60:b3:ac:a1:94	1.0	2412	1.0	104788	4744	0.88	-43.38	-38.78
4	3	4	0:60:b3:b0:c6:41	0:60:b3:ac:a1:94	1.0	2412	0.63	101660	6816	0.87	-45.06	-51.61
5	4	5	0:60:b3:b0:c6:41	0:60:b3:ac:a1:94	1.0	2412	0.75	100096	7752	0.86	-44.37	-35.94
6	5	6	0:60:b3:b0:c6:41	0:60:b3:ac:a1:94	1.0	2412	1.0	95404	7052	0.82	-55.32	-46.28
7	6	7	0:60:b3:b0:c6:41	0:60:b3:ac:a1:94	1.0	2412	0.85	93840	7912	0.81	-61.18	-38.03
8	7	8	0:60:b3:b0:c6:41	0:60:b3:ac:a1:94	1.0	2412	0.54	95404	3944	0.79	-57.08	-37.03
9	8	9	0:60:b3:b0:c6:41	0:60:b3:ac:a1:94	1.0	2412	0.92	98532	3932	0.82	-45.34	-35.45
10	9	10	0:60:b3:b0:c6:41	0:60:b3:ac:a1:94	1.0	2412	1.0	104788	6244	0.89	-47.34	-51.78

Figure 5.3: Snapshot of the link table showing main columns

Bluetooth Interference:

Since Bluetooth only corrupts some packets at random, the transmitter still sees the channel as occupied as before and tries to counter the errors by retransmissions which in turn increases the link occupancy. Thus in this case, there is an increase in both the occupancy as well as the percentage retransmission. In our experiments, we create this case by turning on the Bluetooth link along with the video link. Other 802.11 links (2,3,4 and 5) were also turned on with their nominal traffic flow.

Channel Congestion:

When there are a number of high-speed 802.11 links in the same contention region, each one gets only a fraction of the channel occupancy and also the number of collision induced errors increases substantially following Bianchi's model. [30] Hence this gives rise to a large drop in occupancy accompanied by an increase in the percentage retransmission. We emulate this by turning on all the 802.11 links with 15 Mbps UDP data traffic at 54Mbps link speed.

Slow link on Same AP:

As seen in section 2, a slow link in the network can cause problems for other high-speed links by occupying the shared channel for a large amount of time. This is mostly followed by a slight increase in retransmissions as the number of collisions increase compared to the baseline case. For the emulation, link 2 of Figure 5.1 is converted to a slow 1 Mbps link while all other links carry their normal traffic.

Slow link on Other AP:

In this case, link 4 is made a slow link by changing its transmission rate to 1 Mbps, while the other links still carry the baseline traffic. In this case, we observed that the fall in occupancy is less than that in case of the slow link, same AP case, but the effect on both occupancy and percentage retransmissions is qualitatively the same. This ambiguity between the same AP and other AP cases can be solved by using the information about AP Mac addresses in the diagnosis algorithm.

5.3 Threshold Selection

An important point in the above discussion and in Figure 5.2 is the value of the thresholds that we set to distinguish between different regions. The values specified in Figure 5.2 are heuristic bounds that we observed from repeated trials under different traffic and rate conditions. The thresholds are also chosen relative to the baseline values, Occupancy = p_b and Retransmission percentage = r_b, which makes the thresholds robust for streaming video transmissions of any rate. However, the thresholds, being heuristically derived, are still prone to change based on the topology and the number of interfering devices present in the environment. To make our algorithms work in more generic environments, our next step would be to use Support Vector Machines (SVM) [31] to derive the hyperplanes for multidimensional parameter classification. The basic concept of SVMs involves machine learning based on a set of training set. The training set is used to cluster the observations into different sets to build appropriate hyperplanes. In the online phase, these hyperplanes are used to give a judgment about the new observation based on the model developed out of the training data. Thus the immediate next step in the diagnosis algorithm front would be to use a large set of traces from different topologies, varying the data rates, distance from interferers and traffic patterns, and then setting up a SVM to come up with the required thresholds.

5.4 Experimental Verification

To get an idea about the robustness of the parameters selected and the thresholds derived, we ran a number of experiments for each kind of interference and ran our diagnosis algorithm to determine the problem type in each case. Table 5.1 lists the different configurations that we tested our algorithm on and also shows the minimum, maximum and average values of the two relevant parameters. For the purpose of this experiment, we used the same video link described earlier in the section as the primary link and the baseline values of $r_b = 2.8\%$, $p_b = 0.24$ is used to set the decision thresholds. The interference configurations are as mentioned in the table, for example in the Bluetooth case, we vary the distance between the video receiver and the Bluetooth pair and Table 5.1 shows the corresponding results for distances 1, 6 and 11 meters. Based on the thresholds, the algorithm correctly diagnoses the presence of Bluetooth interference in the first two cases while it fails in the 11m case due to the relatively less impact of the interference on the main link. Similarly, in case of a slow link interference, when the slow link data rate is set to 11 Mbps and its distance from the main link is 15m, the occupancy level goes above the threshold causing the algorithm to incorrectly declare a ‘no-problem’ case. The congestion case is emulated using varying number of extra

Interference Type	% Retransmission			Occupancy			Diagnosis
	Min	Max	Avg	Min	Max	Avg	
Bluetooth - Distance 1m	7.3	21.6	18.0	0.11	0.43	0.39	✓
Bluetooth - Distance 6m	8.1	18.2	16.5	0.14	0.38	0.33	✓
Bluetooth - Distance 11m	4.0	16.1	13.6	0.19	0.26	0.24	x
Slow Link - Rate 1Mbps, Dist 1m	1.7	6.2	4.9	0.01	0.14	0.07	✓
Slow Link - Rate 1Mbps, Dist 15m	0.9	6.1	3.2	0.02	0.19	0.08	✓
Slow Link - Rate 11Mbps, Dist 1m	1.6	8.3	6.5	0.09	0.16	0.12	✓
Slow Link - Rate 11Mbps, Dist 15m	0.9	9.6	7.2	0.12	0.22	0.17	x
Congestion - 4 links, Traffic 20Mbps	11.2	18.0	16.4	0.04	0.12	0.10	✓
Congestion - 4 links, Traffic 5Mbps	7.8	13.7	10.1	0.10	0.21	0.17	x
Congestion - 3 links, Traffic 20Mbps	6.1	14.2	9.8	0.05	0.18	0.12	✓

Table 5.1: Diagnosis Output for the proposed heuristic algorithm over different interference cases

high-speed links and also varying the amount of TCP traffic that each link carries. The traces record an occupancy level of 0.17 in the case of 4 competing links with 5Mbps TCP traffic each and thus fails to diagnose the problem in this case. It can be noted here that in all the 'missed' diagnosis cases, due to the distance and/or the datarate of the interfering link, its effect on the video link is reduced bringing it closer to the baseline operating point and thus making it harder to diagnose. However in these cases, the quality degradation in the video link is also reduced and a potential user of such a system would care less about these cases than those of substantially higher degradations.

Chapter 6

Conclusions and Future Work

Shared use of the unlicensed ISM spectrum, just like any other shared resource is only as good as its rules for fair play and peaceful co-existence. With no means of central control or arbitration between heterogeneous radios, the 2.4 GHz band is gradually becoming interference limited. The experimental results in this thesis outline the impact of inter-radio interference and show that in typical topologies, the effect of one radio class on others causes significant reductions in the throughput. In particular, we show in Section 2 some common scenarios like presence of a slower rate 802.11 link on the same channel as a high rate link, co-located Bluetooth and 802.11 radios, simultaneous transmissions of video-UDP over multiple links and a dense deployment of Bluetooth and ZigBee radios, and benchmark the loss in usable throughput in each case. All of these problems are fairly widespread and limit the quality of service of the applications that run on the wireless system.

Research has outlined many techniques for better co-existence mechanisms and proposals of common shared channel for cooperation. However, the widespread and diverse deployment of different radio devices and the clause of legacy support that any feasible solution should possess, severely limits the use of such corrective systems. In such a scenario, fault diagnosis and detailed interference analysis can lead to an improved use of the shared spectrum and provide the end users of the system with valuable insight to the myriad interference related problems. While a wide variety of tools exists for detailed diagnosis and network monitoring in wired networks, spectrum monitoring techniques for the wireless domain are still underdeveloped. As such, we have outlined some techniques for trace collection and storage in Section 3 which provide a more detailed view of the multi-radio environment. Based on this our work proposes the design of a framework for multi-radio monitoring which provides the basis for an elaborate system for diagnosis of interference related problems. The basic building blocks of the system consists of a set of disparate monitors that employ different means of data collection and a database server that time synchronizes the trace collection process and maintains the different tables for use by the diagnosis algorithm. Having setup such a framework, in future work we will apply data mining techniques that can use trace data from multiple tables and identify problem scenarios for non-trivial cases of multi-radio interference. As such, the design of diagnosis algorithms would first require insights on building theoretical and heuristic models for multi-radio interference and on identifying metrics that can be useful for the diagnosis of interference related problems. Recent advancements in machine learning methods and intelligent algorithms can significantly contribute to this work.

References

[1] G. Hardin, "The tragedy of the commons," *Science*, vol. 162, no. 3859, pp. 1243–1248, December 1968.

[2] P. Weiser and D. Hatfield, "Policing the Spectrum Commons," *Fordham Law Review, Vol. 74*, 2005.

[3] N. Golmie, N. Chevrollier, and O. Rebala, "Bluetooth and WLAN coexistence: Challenges and solutions," *IEEE Wireless Communications Magazine*, vol. 10, pp. 22–29, 2003.

[4] A. Arumugam, A. Doufexi, A. Nix, and P. Fletcher, "An investigation of the coexistence of 802.11g WLAN and high data rate Bluetooth enabled consumer electronic devices in indoor home and office environments," *IEEE Transactions on Consumer Electronics*, vol. 49, no. 3, pp. 587 – 596, Aug. 2003.

[5] S. Y. Shin, H. S. Park, S. Choi, and W. H. Kwon, "Packet error rate analysis of ZigBee under WLAN and Bluetooth interferences," *IEEE Transactions on Wireless Communications*, vol. 6, no. 8, pp. 2825–2830, August 2007.

[6] *IEEE 802.15.2-2003, IEEE Recommended Practice for Information Technology Part 15.2: Coexistence of Wireless Personal Area Networks with Other Wireless Devices Operating in the Unlicensed Frequency Bands*, Std., 2003.

[7] R. Gummadi, D. Wetherall, B. Greenstein, and S. Seshan, "Understanding and mitigating the impact of RF interference on 802.11 networks," in *Proc. of Sigcomm07*, 2007, pp. 385–396.

[8] A. Stranne, O. Edfors, and B.-A. Molin, "Energy-based interference analysis of heterogeneous packet radio networks." *IEEE Transactions on Communications*, vol. 54, no. 4, pp. 761–761, 2006.

[9] X. Jing, S. Anandaraman, M. Ergin, I. Seskar, and D. Raychaudhuri, "Distributed coordination schemes for multi-radio co-existence in dense spectrum environments: An experimental study on the orbit testbed," in *Proc. of DySPAN08*, Oct. 2008, pp. 1–10.

[10] Y.-C. Cheng, M. Afanasyev, P. Verkaik, P. Benkö, J. Chiang, A. C. Snoeren, S. Savage, and G. M. Voelker, "Automating cross-layer diagnosis of enterprise wireless networks," in *Proc. of Sigcomm07*, 2007, pp. 25–36.

[11] A. Adya, P. Bahl, R. Chandra, and L. Qiu, "Architecture and techniques for diagnosing faults in IEEE 802.11 infrastructure networks," in *MobiCom '04: Proceedings of the 10th annual international conference on Mobile computing and networking*, 2004, pp. 30–44.

[12] B. Yan and G. Chen, "Model-based fault diagnosis for IEEE 802.11 wireless LANs," in *Proceedings of the Sixth Annual International Conference on Mobile and Ubiquitous Systems: Computing, Networking and Services (MobiQuitous)*, Toronto, Canada, Jul. 2009, to appear.

[13] J.-H. Yun and S.-W. Seo, "Collision detection based on RF energy duration in IEEE 802.11 wireless lan," in *Communication System Software and Middleware, 2006. Comsware 2006. First International Conference on*, 2006, pp. 1–6.

[14] A. Sheth, C. Doerr, D. Grunwald, R. Han, and D. Sicker, "MOJO: a distributed physical layer anomaly detection system for 802.11 wlans," in *MobiSys '06: Proceedings of the 4th international conference on Mobile systems, applications and services*, 2006, pp. 191–204.

[15] S. Rayanchu, A. Mishra, D. Agrawal, S. Saha, and S. Banerjee, "Diagnosing wireless packet losses in 802.11: Separating collision from weak signal," in *INFOCOM 2008. The 27th Conference on Computer Communications. IEEE*, April 2008, pp. 735–743.

[16] D. Raychaudhuri, I. Seskar, M. Ott, S. Ganu, K. Ramachandran, H. Kremo, R. Siracusa, H. Liu, and M. Singh, "Overview of the orbit radio grid testbed for evaluation of next-generation wireless network protocols," in *Proc. of IEEE Wireless Communications and Networking Conference, 2005*, vol. 3, March 2005, pp. 1664–1669.

[17] J. Polastre, R. Szewczyk, and D. Culler, "Telos: enabling ultra-low power wireless research," in *IPSN '05: Proceedings of the 4th International symposium on Information processing in sensor networks*, 2005.

[18] Iperf network testing tool, http://www.noc.ucf.edu/Tools/Iperf/.

[19] UC Berkeley, "TinyOS Community Forum," http://www.tinyos.net.

[20] N. Golmie, O. Rebala, and N. Chevrollier, "Bluetooth adaptive frequency hopping and scheduling," in *Military Communications Conference, 2003. MILCOM 2003. IEEE*, vol. 2, 2003, pp. 1138 – 1142 Vol.2.

[21] J. Yeo, M. Youssef, and A. Agrawala, "A framework for wireless LAN monitoring and its applications," in *WiSe '04: Proceedings of the 3rd ACM workshop on Wireless security*, 2004, pp. 70–79.

[22] Y. Sheng, G. Chen, H. Yin, K. Tan, U. Deshpande, B. Vance, D. Kotz, A. Campbell, C. McDonald, T. Henderson, and J. Wright, "MAP: A scalable monitoring system for dependable 802.11 wireless networks," *IEEE Wireless Communications*, vol. 15, no. 5, pp. 10–18, October 2008.

[23] Tcpdump packet analyzer application, http://www.tcpdump.org.

[24] R. Miller, W. Xu, P. Kamat, and W. Trappe, "Service discovery and device identification in cognitive radio networks." in *Proc. of IEEE SECON*, 2007, pp. 670–677.

[25] C. Raman, J. Kalyanam, I. Seskar, and N. Mandayam, "Distributed Spatio-Temporal Spectrum Sensing: An Experimental Study," in *Signals, Systems and Computers, 2007. ACSSC 2007. Conference Record of the Forty-First Asilomar Conference on*, Nov. 2007, pp. 2063 –2067.

[26] FTS4BT Bluetooth Protocol Analyzer & Packet Sniffer, Frontline Technology, http://www.fte.com.

[27] Wi-Spy USB Spectrum Analyzer, http://www.metageek.net/products/wi-spy.

[28] M. Singh, M. Ott, I. Seskar, and P. Kamat, "Orbit measurements framework and library (oml): Motivations, design, implementation, and features," in *TRIDENT-COM '05: Proceedings of the First International Conference on Testbeds and Research Infrastructures for the DEvelopment of NeTworks and COMmunities*, 2005, pp. 146–152.

[29] VideoLAN non-profit organisation, "VLC media player: The cross-platform open-source multimedia framework, player and server," http://www.videolan.org/.

[30] G. Bianchi, "Performance Analysis of the IEEE 802.11 Distributed Coordination Function," *IEEE Journal on Selected Areas in Communications*, vol. 18, no. 3, pp. 535–547, October 2000.

[31] C.-C. Chang and C.-J. Lin, *LIBSVM: a library for support vector machines*, 2001, software available at http://www.csie.ntu.edu.tw/ cjlin/libsvm.